第 42 卷第 6 期
2023 年 12 月

红 外 与 毫 米 波 学 报
J. Infrared Millim. Waves

Vol. 42, No. 6
December, 2023

文章编号：1001-9014(2023)06-0779-09 **DOI**：10.11972/j.issn.1001-9014.2023.06.011

Enhanced terahertz wave generation in air-plasma induced by femtosecond three-color harmonic pulses

WANG Han-Qi[1,2], FAN Wen-Hui[1,2,3*], CHEN Xu[1], YAN Hui[1,2]

(1. State Key Laboratory of Transient Optics and Photonics, Xi'an Institute of Optics and Precision Mechanics, Chinese Academy of Sciences, Xi'an 710119, China;
2. University of Chinese Academy of Sciences, Beijing 100049, China;
3. Collaborative Innovation Center of Extreme Optics, Shanxi University, Taiyuan 030006, China)

Abstract: The generation of terahertz waves from air-plasma induced by femtosecond three-color harmonic pulses with a frequency ratio of 1:2:*m* (*m* is a positive integer), based on the transient photocurrent model and the saw-tooth-like electric field formed via multi-color harmonic pulses superposition, has been theoretically investigated. It can be seen that when the air is saturated ionized and the electron density reaches the same maximum, for the same number of harmonic pulses, terahertz conversion efficiency is not always higher when the electric field shape in the composed pulse envelope is closer to a sawtooth waveform and more asymmetric. Besides, the specific wavelength combination schemes of femtosecond three-color harmonic pulses with the frequency ratios of 1:2:3 and 1:2:4 have also been simulated, which can significantly enhance the generation of terahertz waves, and are realized by adding only a set of optical parametric amplifiers on the basis of the conventional two-color laser pulse case at the frequency ratio of 1:2. Our study will be helpful to obtain intense terahertz sources and provide guidance for experimental operations.

Key words: three-color harmonic pulses, air-plasma, wavelength combination scheme, enhanced terahertz wave generation

飞秒三色谐波脉冲增强空气等离子体中太赫兹波的产生

王汉奇[1,2]， 范文慧[1,2,3*]， 陈 徐[1]， 闫 慧[1,2]

(1. 中国科学院西安光学精密机械研究所 瞬态光学与光子技术国家重点实验室，陕西 西安 710119；
2. 中国科学院大学，北京 100049；
3. 山西大学 极端光学协同创新中心，山西 太原 030006)

摘要：本文基于瞬态光电流模型和多色谐波脉冲叠加形成的类锯齿形电场，研究了频率比为1:2:*m*(*m*为正整数)的飞秒三色谐波脉冲诱导空气等离子体产生太赫兹波的情况。结果表明，在空气被饱和电离且电子密度达到相同最大值的情况下，对于相同数量的谐波脉冲，当合成脉冲包络中的电场形状更接近锯齿形且更不对称时，太赫兹波的转换效率并不总是更高。此外，研究了采用频率比为1:2:3和1:2:4的飞秒三色谐波脉冲的特定波长组合方案增强太赫兹波的产生。对于这些特定的波长组合方案，可以在常用频率比为1:2的双色光脉冲方案基础上仅添加一组光参量放大器就能实现。我们的研究将有助于获得强太赫兹波源，并为实验操作提供指导。

关 键 词：三色谐波脉冲；空气等离子体；波长组合方案；增强太赫兹波产生

中图分类号：O434.3 **文献标识码**：A

Received date: 2023-02-20, **revised date**: 2023-04-13 **收稿日期**：2023-02-20，**修回日期**：2023-04-13

Foundation items: Supported by the National Natural Science Foundation of China (61675230, 61905276); the Natural Science Foundation of Shaanxi Province (2020JQ-437); and the Open Research Fund of Key Laboratory of Spectral Imaging Technology, Chinese Academy of Sciences (LSIT201913N)

Biography: Wang Han-Qi, male, Xinzhou Shanxi, Ph. D. Research area involves terahertz waves generation and application. E-mail: whqwanghanqi@163.com

[*] **Corresponding author**: E-mail: fanwh@opt.ac.cn

Introduction

Terahertz (THz) waves have attracted significant attention in the fields of physics, chemistry, physiology and medicine [1-7]. The acquisition of intense THz sources is of important significance for the practical application of THz waves. Intense THz waves can be generated in air-plasma induced by femtosecond laser pulses, but whether it is a one-color laser pulse scheme or a two-color laser (fundamental and its second harmonic) pulse scheme, the generation efficiency of THz waves is relatively low [8, 9]. Some research groups have tried to increase the output of THz waves in different ways, for example, adjusting the laser polarization, phase, wavelength, pulse duration, electric field amplitude ratio and frequency ratio[10-16], varying the gas composition and pressure[17, 18], altering the plasma shape and density distribution[19, 20], adding the external field[21, 22], and so on. In 2015, Martínez *et al.* demonstrated when the number of femtosecond laser harmonic pulses participating in the nonlinear interaction increases and the electric field shape formed via the superposition of multi-color harmonic pulses is sawtooth-like shape, multi-color harmonic pulse scheme can have higher yield of THz waves compared with that by the one-color laser pulse scheme and the two-color laser pulse scheme [23]. Several research groups have also proposed some wavelength combination schemes by using multi-color harmonic pulses or multi-color non-harmonic pulses to generate intense THz waves and even carried out relevant experiments [24-33]. However, the interesting issue on how to design the frequency ratio and the wavelength combination scheme of multi-color pulses more suitably still needs to be further explored.

In the paper, based on the sawtooth-like electric field formed via femtosecond multi-color harmonic pulse superposition and the conventional scheme that femtosecond two-color laser pulses at the frequency ratio of 1:2 excite the air-plasma to radiate THz waves experimentally, we theoretically investigated the variation trends of THz wave generation by femtosecond three-color harmonic pulses with the frequency ratio of 1:2:*m* ($3\leqslant m\leqslant 20$) according to the transient photocurrent model (TPCM), and distinguished the similarity between the electric field shape of the composed pulse and the perfect sawtooth waveform by a simple and efficient method. The results reveal when the electric field shape in the composed pulse envelope is closer to the sawtooth waveform and more asymmetric, the THz conversion efficiency is not always higher for the same number of harmonic pulses. The specific wavelength combination schemes of three-color harmonic pulses at the frequency ratios of 1:2:3 and 1:2:4 have been also studied and presented. These specific wavelength combination schemes can significantly enhance the THz wave generation, and be achieved by adding only a set of optical parametric amplifiers (OPA) on the basis of the conventional two-color laser pulse case at frequency ratio of 1:2. In addition, we demonstrate when the relative phase of the highest harmonic is varied, the maximum THz yield of the three-color pulse scheme at the frequency combination of 1:2:4 is slightly smaller than that of the three-color pulse case at the frequency combination of 1:2:3, but its overall THz yield can be maintained better stability and smaller fluctuation. When the amplitude ratio of the highest harmonic is appropriately increased, the three-color pulse scheme at the frequency combination of 1:2:4 can generate stronger THz waves than that of the three-color pulse case at the frequency combination of 1:2:3.

1 Theoretical methods

As a theoretical mechanism of THz wave generation in air-plasma excited via femtosecond two-color laser pulses, the TPCM can also be applied to the analysis of multi-color harmonic pulse schemes [23]. It is assumed that all the harmonic pulses involved have the same polarization and pulse duration. Firstly, the sawtooth-like electric field $E(t)$ based on multi-color harmonic pulse superposition can be expressed as [23]

$$E(t)=\sum_{n=1}^{N}\frac{1}{n}E_0\cos\left[\omega_n t+(-1)^n\left(\frac{\pi}{2}\right)\right]\exp\left(\frac{-2\ln 2t^2}{\tau^2}\right)\quad,\quad(1)$$

where N is the number of multi-color harmonic pulses, E_0 is the electric field amplitude, ω_n is the central frequency of each pulse, τ is the pulse duration. Then, according to the TPCM, the composed pulse ionizes air to form an air-plasma. The type of ionization can be classified by the Keldysh parameter [34]

$$\gamma=\frac{\omega}{e}\sqrt{\frac{2m_e U_P}{U}}\quad,\quad(2)$$

where e is the electron charge, ω is the frequency of the laser, m_e is the electron mass, U is the laser pulse induced ponderomotive potential, U_P is the ionization potential of the gas. When $\gamma\ll 1$, the main ionization mechanism is tunnel ionization and the ionization rate can be expressed as [11-13]

$$r(t)=4\omega_a\left[\frac{E_a}{E(t)}\right]\exp\left[-\frac{2}{3}\frac{E_a}{E(t)}\right]\quad,\quad(3)$$

where ω_a is the atomic frequency unit, E_a is the atomic unit of the electric field. By tunnel ionization, bound electrons move away from the neutral gas particle as the Coulomb barrier is suppressed by the instantaneous electric field of the composed pulse, a large number of free electrons will be produced, and the time-varying electron density is given by [11-13]

$$\frac{d\rho_e(t)}{dt}=\left[\rho_g-\rho_e(t)\right]r(t)\quad,\quad(4)$$

where $\rho_e(t)$ is the electron density, ρ_g is the neutral gas density. Then, the free electrons will drift under the electric field of the composed pulse. The drift velocity $\upsilon_e(t)$ is [11-13]

$$\upsilon_e(t)=-\frac{e}{m_e}\int_{t'}^{t}E(t)dt\quad,\quad(5)$$

where t' is the time to produce free electrons. The drifting motion of free electrons will generate a photocurrent, and the time-varying photocurrent density $dJ(t)/dt$ is presented as [11-13]

$$\frac{dJ(t)}{dt} = e\frac{d\rho_e(t)}{dt}\upsilon_e(t) - \nu_c J(t) \quad , \quad (6)$$

where ν_c is the collision frequency of electron-ion and electron-neutral particle. The pulse duration is much shorter than the average collision time between particles, so the collision frequency can be ignored. Finally, the time-varying photocurrent density generates THz waves. The electric field amplitude of THz waves can be expressed as [11-13]

$$E_{THz} \propto \frac{dJ(t)}{dt} \quad . \quad (7)$$

2 Results and discussion

According to Eq. (1), if the parameter N becomes larger, the more harmonic pulses will participate in the nonlinear interaction, the shape of the electric field formed via the superposition of multi-color harmonic pulses will become closer to the perfect sawtooth waveform, and THz waves will be more strongly generated [23]. However, in practice, due to the limitation of cost, equipment volume, energy consumption and operation complexity, we can only operate a finite number of harmonic pulses. Therefore, the appropriate pulse number and pulse frequency (wavelength) should be chosen carefully. On the basis of the current two-color pulse case at the frequency ratio of 1∶2, it is more feasible to add one more color pulse to form three-color harmonic pulses with the frequency ratio of 1∶2∶m (m≥3), where m is the frequency ratio of the corresponding third color harmonic pulse and is a positive integer.

Thus, we calculate the electric field peak-peak amplitude of THz pulse radiated from femtosecond three-color harmonic pulses with the frequency ratio of 1∶2∶m (3≤m≤20), and compare them with that generated by the two-color pulse case, as shown in Fig. 1. Note, when m=2, it indicates the two-color pulse case at the frequency combination of 1∶2, not 1∶2∶2. In the calculation, for three-color harmonic pulse schemes, we assume that the total peak power density is 5×10^{14} W/cm^2 within the laser intensity clamping regime, the fundamental wavelength is 1600 nm, the pulse duration is 50 fs, the amplitude ratio and phase of each pulse are strictly determined according to the parameters in Eq. (1). For the two-color pulse scheme, the peak power density, the fundamental wavelength and the pulse duration are identical with three-color harmonic pulse schemes, the amplitude ratio is also determined by Eq. (1), but the relative phase is assigned as $\pi/2$ that can generate the strongest THz pulse[11]. The results show, when the frequency ratio is 1∶2∶3, the strongest THz pulse is radiated; when the frequency ratio is 1∶2∶4, its yield of THz waves takes the second place; and THz waves are much more powerful when output via three-color harmonic pulses at these two frequency ratios compared with that generated via the two-color pulses at the frequency ratio of 1∶2. When the frequency combination is 1∶2∶5, the THz yield is the smallest. After the frequency ratio of 1∶2∶10, the output of THz waves gradually tends to weakly stable and equivalent to the result of two-color pulse scheme. This is because along with the increase of parameter "m" in Eq. (1), the electric field amplitude ratio of the third color harmonic pulse rapidly decreases according to the reciprocal of parameter "m", and harmonic order becomes larger and larger, the effect of the third color pulse on the THz wave generation becomes weaker and weaker.

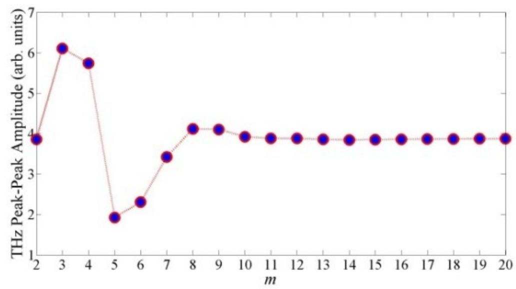

Fig. 1 The THz electric field peak-peak amplitude of three-color harmonic pulse schemes with the frequency ratio of 1∶2∶m (3≤m≤20), when m=2, it indicates the two-color pulse case at the frequency ratio of 1∶2, red dot lines connecting data (blue) are used to guide vision only and do not mean anything

图1 频率比为1∶2∶m(3≤m≤20)的三色谐波脉冲方案产生的太赫兹波电场峰峰值,当m=2时,表示频率比为1∶2的双色脉冲方案,连接数据点(蓝色)的红色点线仅用于视觉引导,不代表任何物理意义

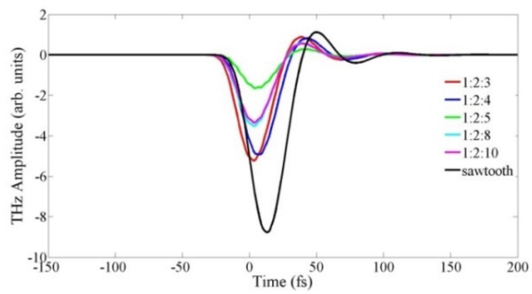

Fig. 2 The time-domain waveform of THz waves generated from three-color harmonic pulse schemes at different frequency ratios and the pulse scheme containing the perfect sawtooth electric field, respectively

图2 不同频率比的三色谐波脉冲方案和包含完美锯齿形电场的脉冲方案产生的太赫兹波时域波形

In order to explore the different THz wave output from three-color harmonic pulse cases at various frequency ratios, we select several typical frequency ratios as research objects. Figure 2 shows the time-domain waveform of THz pulses generated from three-color harmonic pulse schemes at typical frequency combinations of 1∶2∶3, 1∶2∶4, 1∶2∶5, 1∶2∶8, 1∶2∶10, and sawtooth waveform, respectively. After the relevant air parameters such as air type and concentration are fixed, the electric field formed via the superposition of multi-color harmonic pulses will play a decisive role in the generation of THz waves. Figure 3(a) displays the composed pulse envelope containing several electric field oscillation periods at typical frequency ratios and sawtooth waveform. To clearly observe the structure of the electric field, in Fig. 3(b), we display the electric field oscillation period in the time range of -6 fs to 6 fs in the composed pulse envelope. It is considered that the number of harmonics is larger, the electric field shape is closer to the sawtooth waveform, resulting in the higher THz yield, when the ionization yield or the pump energy flux is identical [23]. Then, for the same number of harmonic pulses, is the THz conversion efficiency also higher when the electric field shape is closer to sawtooth waveform? In Fig. 3, however, it is difficult to intuitively judge which electric field shape is closer to the sawtooth waveform. Some parameters can characterize the electric field shape, including the slope of the rising edge and the falling edge, the envelope area difference between the left and right sides of the peak, the peak-peak amplitude difference, the time difference between the adjacent peaks, and so on. Here, we take a simple and effective quantitative approach related to the time interval to compare the electric field shape, and describe the dependence of THz wave generation on the electric field structure of the composed pulse.

Both the electron drift velocity and the time-varying electron density are important parameters related to the THz yield and determined by the electric field of the composed pulse. The electron drift velocity represents the ability to drift away from their parent ions. The electron drift velocity also contains the information on both the shape and asymmetry of the electric field of the composed pulse [23]. In Fig. 4, we present the electric field, electron drift velocity, and ionization rate of typical frequency ratios and sawtooth waveform in the time range of -21 fs to -10 fs before saturation ionization, respectively. The each peak electric field of the composed pulse is extremely important for the analysis of THz wave generation. The values of the ionization rate indicate the ionization mainly occurs within the full width at half maximum (FWHM) of electric field corresponding to the shadowed area in Fig. 4, and reach the extreme value at the same time as the electric field. The drift velocity of electrons born with opposite signs will be cancelled, and only the net electron drift velocity within the FWHM of each electric field contributes to the THz wave generation [11]. Ideally, in order to maximize the net electron drift velocity, the velocity should remain the extreme value and have the same sign during ionization [23].

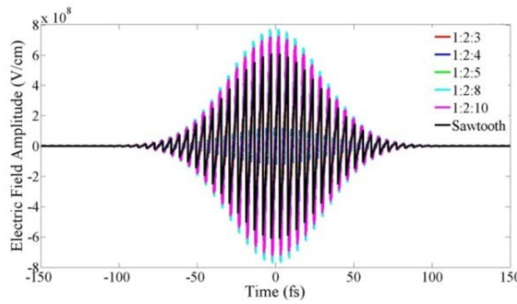

(a)

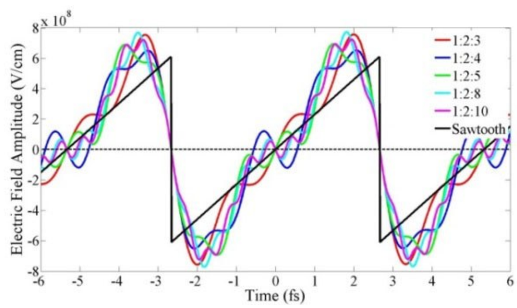

(b)

Fig. 3 (a) The pulse envelope composed by three-color harmonic pulses at different frequency ratios, and the pulse envelope containing the perfect sawtooth electric field, respectively, (b) the electric field structure in the time range of -6 fs to 6 fs in the composed pulse envelope, the black dashed line is the grid line

图3 (a)不同频率比的三色谐波脉冲合成的光脉冲包络和包含完美锯齿形电场的光脉冲包络,(b)合成脉冲包络中-6 fs至6 fs时间范围内的电场结构,黑色虚线是网格线

For the sawtooth-like electric field of each frequency ratio, the electric field peak and the electron drift velocity peak are out of sync, ionization is interrupted before the velocity reaches the peak, and the velocity during ionization can be obviously divided into two parts according to the positive and negative signs, as shown in Figs. 4(a), (b), (c), (d) and (e). The asynchrony is not conductive to add the net electron drift velocity. However, for the sawtooth waveform, the electric field peak and the electron drift velocity peak are staying in sync during the period of ionization. Figure 4(f) shows when the electric field changes the sign, the ionization maintains continuity so that the drift velocity can attain the extreme value during ionization, and most of the velocities during ionization have the same sign. Therefore, in order to judge which waveform is closer to the sawtooth waveform and more asymmetric, it is reasonable to directly compare the time interval between the electric field peak and the adjacent velocity peak. When the time interval is shorter, the net electron drift velocity will be larger, and the electric field shape will become closer to the sawtooth waveform and more asymmetric.

We mark the time corresponding to the electric field peak and the adjacent velocity peak with two black dashed lines perpendicular to the time axis in Fig. 4. The detailed time interval between the electric field peak and the adjacent velocity peak at different frequency ratios is shown in Table 1. It is found for three-color harmonic pulses with the frequency ratio of $1:2:m$, the THz conversion efficiency is not always higher when the time interval is shorter and the electric field shape is closer to the sawtooth waveform. Besides, based on the periodic oscillation characteristics of the electric field, ionization rate and velocity, the electron drift velocity reaches the local extreme value when the rising and falling edges of the electric field change their signs, we can also judge the approximation level between the electric field shape

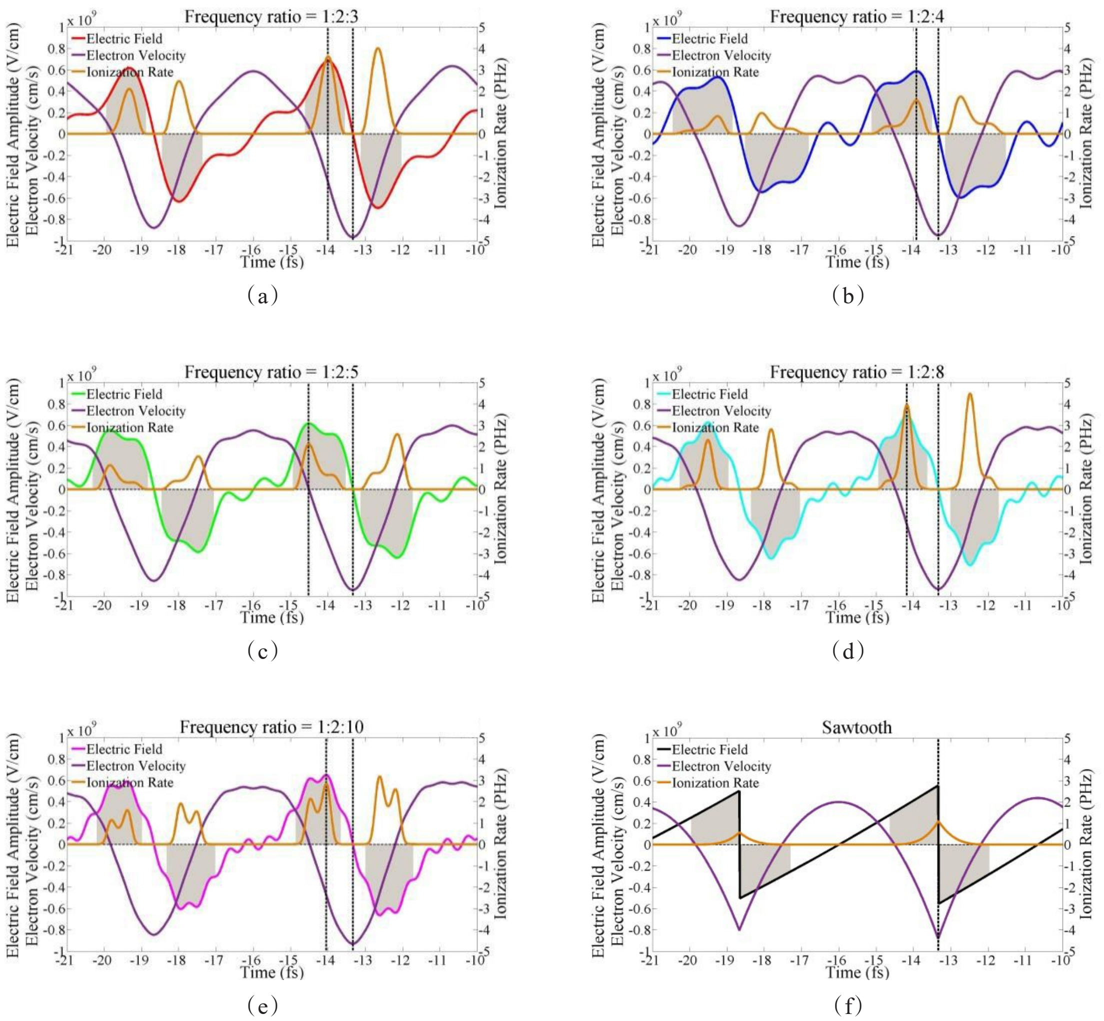

Fig. 4 In the time range of -21 fs to -10 fs, the electric field structure, electron drift velocity, and ionization rate corresponding to the pulse composed by three-color harmonic pulses at different frequency ratios and the pulse containing the perfect sawtooth electric field, (a) 1:2:3, (b) 1:2:4, (c) 1:2:5, (d) 1:2:8, (e) 1:2:10, (f) the perfect sawtooth electric field, respectively
图4 在-21 fs到-10 fs的时间内,不同频率比的三色谐波脉冲叠加合成的光脉冲和包含完美锯齿形电场的光脉冲对应的电场结构、电子漂移速度和电离率,(a) 1:2:3,(b)1:2:4,(c)1:2:5,(d)1:2:8,(e)1:2:10,(f)完美锯齿形电场

and the sawtooth waveform by comparing the time interval between the positive peak and the negative peak on the rising edge of the electric field, or the time interval between the positive peak and the negative peak on the falling edge of the electric field. It is equivalent to the time interval between the electric field peak and the velocity peak.

Table 1 The time interval between the electric field peak of the composed pulse and the adjacent velocity peak
表1 合成脉冲中电场峰值和相邻速度峰值之间的时间间隔

Frequency ratio	1:2:3	1:2:4	1:2:5	1:2:8	1:2:10	sawtooth
Time interval (fs)	0. 67	0. 59	1. 19	0. 85	0. 72	0

The time-varying electron density and ionization rate represent the ability to produce electrons. Figure 4 shows the ionization mainly depends on the electric field distribution near the peak. Figure 5 further displays the time-varying electron density during the pulse duration at the typical frequency ratios and the sawtooth waveform. Obviously, with the previous assumed laser parameters, the electron density finally reaches the same maximum in the form of stepwise increase at all frequency ratios, and the gas is saturated ionized near the peak of the composed pulse envelope, but the time to complete saturation ionization is different at different frequency ratios. As a result, for the same number of harmonic pulses, the THz yield cannot be directly evaluated from the approximation level between the electric field shape and the sawtooth waveform or from the asymmetric level of the electric field. It is necessary to consider contributions from both the growing electron density and the net electron drift velocity to the generation of the net electron current at the same time. Figure 6 displays the time-varying electron current density of three-color harmonic pulse schemes at different frequency ratios. According to the

TPCM, when the net electron current becomes bigger, the generated THz waves will become stronger.

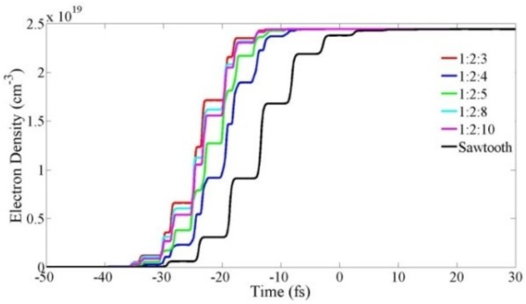

Fig. 5 The time-varying electron density of three-color harmonic pulse schemes at different frequency ratios and the pulse scheme containing the perfect sawtooth electric field, respectively
图5 不同频率比的三色谐波脉冲方案和包含完美锯齿形电场的脉冲方案对应的时变电子密度

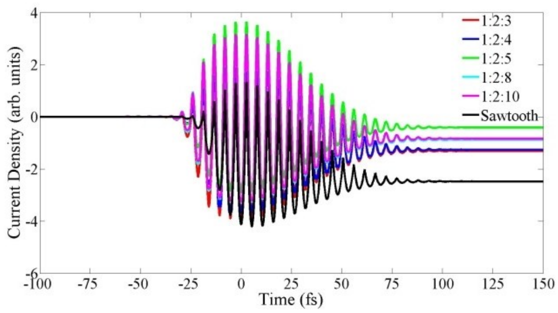

Fig. 6 The time-varying current density of three-color harmonic pulse schemes at different frequency ratios, and the pulse scheme containing the perfect sawtooth electric field, respectively
图6 不同频率比的三色谐波脉冲方案和包含完美锯齿形电场的脉冲方案对应的时变电流密度

Next, it is considered how to design the wavelength combination scheme of three-color harmonic pulses in the actual operation suitably. At present, for the wavelength combination of the two-color pulse scheme, the basic experimental setup is usually a set of a femtosecond laser amplifier system that can generate 800 nm pulse and a β-barium borate (BBO) crystal that can partially double the frequency of 800 nm pulse to the frequency of 400 nm pulse, then the two-color pulses of 800 nm + 400 nm combination are focused into the air and induced air-plasma to generate THz waves. On the basis of the experimental equipment used in the conventional two-color pulse scheme and the calculation results of 1:2:m, we simulate several specific wavelength combination schemes of femtosecond three-color harmonic pulses at the frequency ratios of 1:2:3 and 1:2:4 which can generate intense THz waves. Subject to the above given pump pulse parameters, Fig. 7 shows the time-domain waveform of THz waves generated by 800 nm + 400 nm + 267 nm combination (red dashed line) and 2400 nm + 1200 nm + 800 nm combination (red solid line) at the frequency ratio of 1:2:3, 800 nm + 400 nm + 200 nm combination (blue dot line), 1600 nm + 800 nm + 400 nm combination (blue dashed line) and 3200 nm + 1600 nm + 800 nm combination (blue solid line) at the frequency ratio of 1:2:4, respectively. These wavelength combination schemes can be realized by adding only a set of OPA on the basis of the conventional two-color laser pulse case at the frequency ratio of 1:2. Note that in all wavelength combinations, one color is 800 nm, and the other colors are generated by OPA or BBO crystals. The selection of the frequency ratios of 1:2:3 and 1:2:4 can also facilitate OPA tuning in a limited range. The time-domain waveform of the THz waves generated by 800 nm + 400 nm combination (cyan solid line) at the frequency ratio of 1:2 is provided for comparison. In addition, the THz wave generation by 800 nm + 533 nm + 400 nm combination (green dashed line) and 1200 nm + 800 nm + 600 nm combination (green solid line) in the case of 2:3:4 is also compared, because it can also be achieved by the same experimental equipment as mentioned above. Table 2 further shows the detailed parameters of these wavelength combination schemes.

By comparison, it can be seen the wavelength combination of 3 200 nm+1 600 nm+800 nm can generate extremely intense THz waves at the corresponding frequency ratio of 1:2:4, the second is from the wavelength combination of 2 400 nm+1 200 nm+800 nm at the frequency ratio of 1:2:3, the third is from the wavelength combination of 1 600 nm+800 nm+400 nm at the frequency ratio of 1:2:4. As for the wavelength combination of 800 nm+400 nm+267 nm at the frequency ratio of 1:2:3, and the wavelength combination of 800 nm+400 nm+200 nm at

Table 2 The detailed parameters of THz waves generated by different wavelength combination schemes
表2 不同波长组合方案产生太赫兹波的详细参数

Frequency ratio	Wavelength combination (nm)	THz peak-peak electric field amplitude (arb. units)	Approximate THz amplitude ratio for 800+400 nm combination
1:2	800+400	1. 939 5	1
1:2:3	800+400+267	3. 055 2	1. 57
1:2:3	2 400+1 200+800	9. 117 9	4. 70
1:2:4	800+400+200	2. 900 7	1. 50
1:2:4	1 600+800+400	5. 742 6	2. 96
1:2:4	3 200+1600+800	11. 970 9	6. 17
2:3:4	800+533+400	1. 383 3	0. 71
2:3:4	1 200+800+600	1. 909 9	0. 98

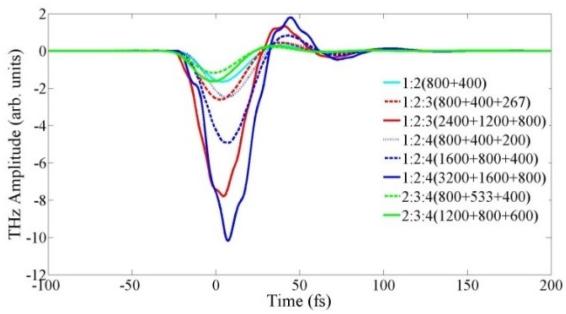

Fig. 7 The time-domain waveform of THz waves generated by different wavelength combination schemes
图7 不同波长组合方案产生的太赫兹波时域波形

the frequency ratio of 1∶2∶4, the output THz waves from them are also stronger than that from the two-color combination of 800 nm+400 nm. When the frequency ratio is 2∶3∶4, the yields of THz waves generated by both 800 nm+533 nm+400 nm combination and 1 200 nm+800 nm+600 nm combination are weaker than that generated by two-color combination of 800 nm+400 nm, so these two wavelength combinations can be excluded.

In addition, with the number of the harmonic pulses increasing, it is recognized that the control of relevant parameters becomes more complex when the requirements of forming the sawtooth-like electric field are met, for example, proportional control, phase control, etc. Overcoming these difficulties depends on the satisfactory experimental equipment and the excellent experimental skill. We have known the 800 nm + 400 nm + 267 nm combination scheme at the frequency ratio of 1∶2∶3 is attempted to output intense THz waves via continuously doubling the frequency for 800 nm pulse with the double BBO crystal instead of OPA and modulating the phase using a phase compensation device with attosecond precision [24, 35, 36], but the configuration of the double BBO crystal has disadvantages of complex operation and poor flexibility. We have also noticed recently some wavelength combination schemes of three-color pulses based on OPA are proposed and relevant experiments are even carried out [26-28]. Hence, the presented wavelength combination schemes are suitable.

Here, it should be noted that not only the selection of frequency ratio can affect the THz wave generation, but also the use of longer wavelength combination can optimize the THz yield. From the perspective of electric field structure, the longer wavelength can also change the electric field structure in the composed pulse. It is similar to the two-color pulse scheme, with longer wavelengths increasing the THz wave output. We take 800 nm+400 nm+200 nm combination, 1 600 nm+800 nm+400 nm combination and 3 200 nm+1 600 nm+800 nm combination at the frequency ratio of 1∶2∶4 as examples. With the increase of wavelength, Fig. 8 shows the number of the electric field oscillation decreases and the period of electric field oscillation increases in the composed pulse envelope. This indicates the effective time of the nonlinear interaction between the pulse and the gas becomes longer, the nonlinear interaction becomes stronger, and THz waves can be more strongly generated.

In previous studies, the electric field amplitude ratio, relative phase, and duration of three-color pulses are determined according to Eq. (1). In practice, these parameters may change due to external influences. Here, the three-color pulse schemes with frequency ratios of 1∶2∶3 and 1∶2∶4 can generate intense THz waves, and the configurations of their first two color pulses are consistent. We focus on the dependence of the THz electric field peak-peak amplitude on the parameters of their highest harmonic, and compare with that generated by the two-color pulse scheme with the frequency ratio of 1∶2. In the calculation, it is assumed that the fundamental wavelength is 800 nm. Figure 9 (a) shows that when the relative phase of the highest harmonic is varied, the maximum THz yield of the three-color pulse scheme at the frequency combination of 1∶2∶4 is slightly smaller than that of the three-color pulse case at the frequency combination of 1∶2∶3, but its overall THz yield can be maintained the better stability and the smaller fluctuation. This is very important for the stable output of THz waves in the real setup. Figure 9 (b) displays that when the amplitude ratio of the highest harmonic is appropriately increased, the three-color pulse scheme at the frequency combination of 1∶2∶4 can generate stronger THz waves than that of the three-color pulse case at the frequency

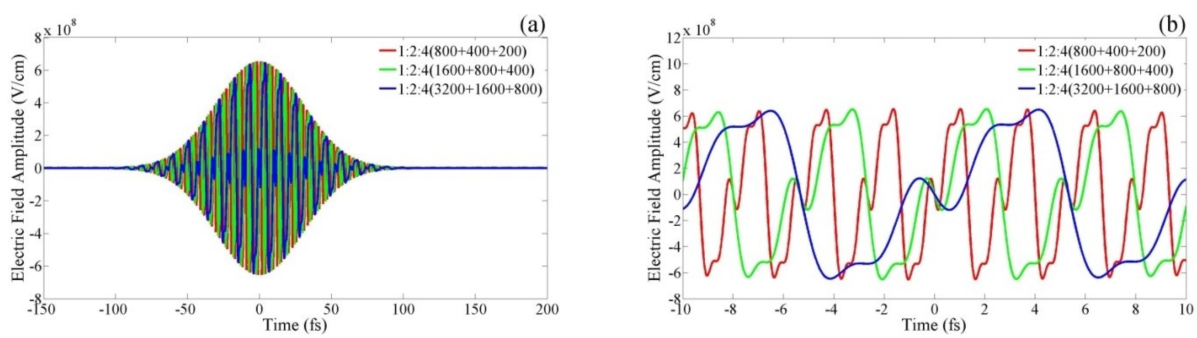

Fig. 8 (a) The pulse envelope composed of different wavelength combinations at the frequency ratio of 1:2:4, respectively, (b) the electric field structure in the time range of -10 fs to 10 fs in the composed pulse envelope
图8 (a)频率比为1:2:4的不同波长组合方案合成的脉冲包络,(b)合成脉冲包络中-10 fs至10 fs时间范围内的电场结构

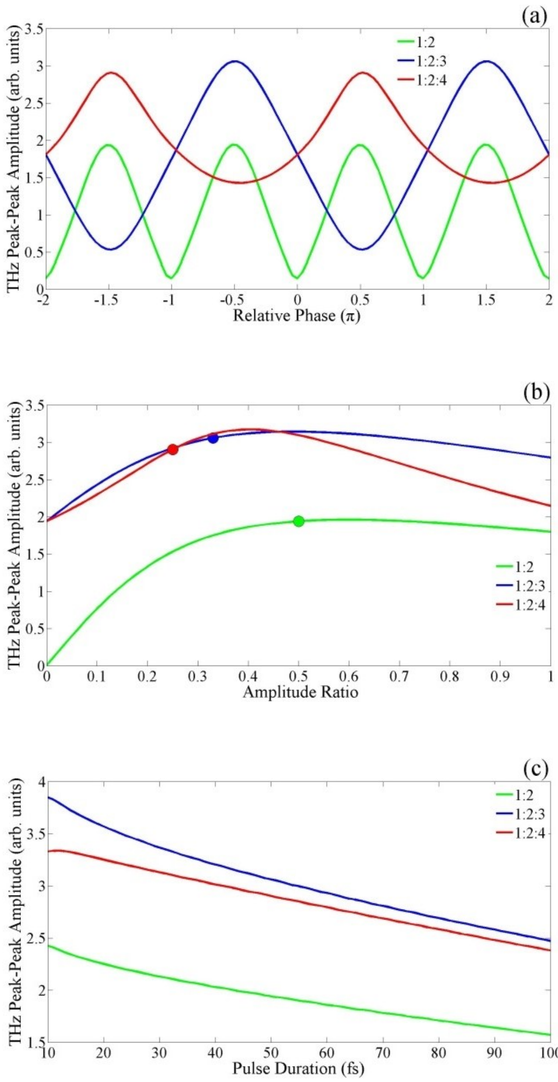

Fig. 9 The dependence of the THz electric field peak-peak amplitude on the parameters of the highest harmonic at frequency ratios of 1:2, 1:2:3 and 1:2:4, including (a) the relative phases, (b) the amplitude ratio, (c) the pulse duration, respectively, the circle dots in (b) correspond to the electric field amplitude ratio of the highest harmonic for three-color pulses in Eq. (1)

图9 太赫兹波电场峰峰值随频率比为1:2、1:2:3和1:2:4的光脉冲方案最高次谐波参数变化的关系,包括(a)相对相位,(b)幅值比,(c)脉宽,(b)中的圆点与公式(1)中三色光脉冲最高次谐波的电场幅值比相对应

combination of 1:2:3. In Fig. 9(c), for both frequency combinations of 1:2:3 and 1:2:4, when the pulse duration of the highest harmonic becomes shorter, the generated THz waves become stronger. On the contrary, the output THz waves gradually decrease.

3 Conclusions

The THz wave generation from the air-plasma induced via femtosecond three-color harmonic pulses with frequency ratios of 1:2:*m* (*m* is a positive integer) has been investigated based on the TPCM and the sawtooth-like electric field formed via the multi-color harmonic pulse superposition. It shows that when the air is saturated ionized and the electron density reaches the same maximum, for the same number of harmonic pulses, the THz conversion efficiency is not always higher when the electric field shape in the composed pulse envelope is closer to the sawtooth waveform and more asymmetric. Furthermore, we present several specific wavelength combination schemes of femtosecond three-color harmonic pulses, which are 800 nm+400 nm+267 nm combination and 2 400 nm+1 200 nm+800 nm combination at the frequency ratio of 1:2:3, 800 nm + 400 nm + 200 nm combination, 1 600 nm+800 nm+400 nm combination and 3 200 nm+1 600 nm+800 nm combination at the frequency ratio of 1:2:4, respectively. These specific wavelength combination schemes can significantly enhance the THz wave generation by adding only a set of OPA on the basis of the conventional two-color laser pulse scheme. This optimization of the THz yield is related to both the selection of frequency ratio and the longer wavelength combination. With the progress of laser technology, we believe the three-color scheme and even the multi-color scheme will become the more effective way to generate intense THz waves. Finally, we demonstrate when the relative phase of the highest harmonic is varied, the maximum THz yield of the three-color pulse scheme at the frequency combination of 1:2:4 is slightly smaller than that of the three-color pulse case at the frequency combination of 1:2:3, but its overall THz yield can be maintained the better stability and the smaller fluctuation. When the amplitude ratio of the highest harmonic is appropriately increased, the three-color pulse scheme at the frequency combination of 1:2:4 can generate stronger THz waves than that of the three-color pulse case at the frequency combination of 1:2:3. Our study will be helpful to obtain intense THz sources and provide guidance for practical operations.

References

[1] Tonouchi M. Cutting-edge terahertz technology [J]. *Nat. Photonics*, 2007, **1**(2): 97-105.

[2] Davies A G, Burnett A D, Fan W H, *et al*. Terahertz spectroscopy of explosives and drugs [J]. *Mater. Today*, 2008, **11**(3): 18-26.

[3] Blanchard F, Doi A, Tanaka T, *et al*. Real-time terahertz near-field microscope [J]. *Opt. Express*, 2011, **19**(9): 8277-8284.

[4] Kampfrath T, Tanaka K, Nelson K A. Resonant and nonresonant control over matter and light by intense terahertz transients [J]. *Nat. Photonics*, 2013, **7**(9): 680-690.

[5] Zhang X C, Shkurinov A, Zhang Y. Extreme terahertz science [J]. *Nat. Photonics*, 2017, **11**(1): 16-18.

[6] Du H W. Systematical study on the role of laser second harmonic generation in the terahertz air coherent detection [J]. *Opt. Laser Technol.*, 2020, **130**: 106312.

[7] Zhang D F, Kroh T, Ritzkowsky F, *et al*. THz-Enhanced DC Ultrafast Electron Diffractometer [J]. *Ultrafast Science*, 2021, 2021(2): 1-7.

[8] Hamster H, Sullivan A, Gordon S, *et al*. Subpicosecond, electromagnetic pulses from intense laser-plasma interaction [J]. *Phys. Rev. Lett.*, 1993, **71**(17): 2725-2728.

[9] Cook D J, Hochstrasser R M. Intense terahertz pulses by four-wave rectification in air [J]. *Opt. Lett.*, 2000, **25**(16): 1210-1212.

[10] Xie X, Dai J M, Zhang X C. Coherent Control of THz Wave Generation in Ambient Air [J]. *Phys. Rev. Lett.*, 2006, **96**(7): 075005.

[11] Kim K Y, Glownia J H, Taylor A J, *et al*. Terahertz emission from ultrafast ionizing air in symmetry-broken laser fields [J]. *Opt. Express*, 2007, **15**(8): 4577-4584.

[12] Kim K Y, Taylor A J, Glownia J H, *et al*. Coherent control of terahertz supercontinuum generation in ultrafast laser - gas interactions [J]. *Nat. Photonics*, 2008, **2**(10): 605-609.
[13] Kim K Y. Generation of coherent terahertz radiation in ultrafast laser-gas interactions [J]. *Phys. Plasmas*, 2009, **16**(5): 056706.
[14] Oh T I, You Y S, Kim K Y. Two-dimensional plasma current and optimized terahertz generation in two-color photoionization [J]. *Opt. Express*, 2012, **20**(18): 19778.
[15] Nguyen A, Kaltenecker K J, Delagnes J C, *et al*. Wavelength scaling of terahertz pulse energies delivered by two-color air plasmas [J]. *Opt. Lett.*, 2019, **44**(6): 1488-1491.
[16] Zhang L L, Wang W M, Wu T, *et al*. Observation of Terahertz Radiation via the Two-Color Laser Scheme with Uncommon Frequency Ratios [J]. *Phys. Rev. Lett.*, 2017, **119**(23): 235001.
[17] Yoo Y J, Jang D, Kim K Y. Highly enhanced terahertz conversion by two-color laser filamentation at low gas pressures [J]. *Opt. Express*, 2019, **27**(16): 22663-22673.
[18] Kim K Y, Glownia J H, Taylor A J, *et al*. High-power broadband terahertz generation via two-color photoionization in gases [J]. *IEEE J. Quantum Electron.*, 2012, **48**(6): 797-805.
[19] Kuk D, Yoo Y J, Rosenthal E W, *et al*. Generation of scalable terahertz radiation from cylindrically focused two-color laser pulses in air [J]. *Appl. Phys. Lett.*, 2016, **108**(12): 121106.
[20] Zhao J Y, Guo L J, Chu W, *et al*. Simple method to enhance terahertz radiation from femtosecond laser filament array with a step phase plate [J]. *Opt. Lett.*, 2015, **40**(16): 3838-3841.
[21] Houard A, Liu Y, Prade B, *et al*. Strong Enhancement of Terahertz Radiation from Laser Filaments in Air by a Static Electric Field [J]. *Phys. Rev. Lett.*, 2008, **100**(25): 255006.
[22] Wang T J, Ju J J, Liu Y X, *et al*. Waveform control of enhanced THz radiation from femtosecond laser filament in air [J]. *Appl. Phys. Lett.*, 2017, **110**(22): 221102.
[23] Martínez P G d A, Babushkin I, Bergé L, *et al*. Boosting Terahertz Generation in Laser-Field Ionized Gases Using a Sawtooth Wave Shape [J]. *Phys. Rev. Lett.*, 2015, **114**(18): 183901.
[24] Petersen P B, Tokmakoff A. Source for ultrafast continuum infrared and terahertz radiation [J]. *Opt. Lett.*, 2010, **35**(12): 1962-1964.
[25] Lu C H, Zhang C Y, Zhang L Q, *et al*. Modulation of terahertz-spectrum generation from an air plasma by tunable three-color laser pulses [J]. *Phys. Rev. A*, 2017, **96**(5): 053402.
[26] Bagley J D, Moss C D, Sorenson S A, *et al*. Laser-induced plasma generation of terahertz radiation using three incommensurate wavelengths [J]. *J. Phys. B At. Mol. Opt. Phys.*, 2018, **51**(14): 144004.
[27] Vaičaitis V, Balachninaite O, Morgner U, *et al*. Terahertz radiation generation by three-color laser pulses in air filament [J]. *J. Appl. Phys.*, 2019, **125**: 173103.
[28] Ma D N, Dong L Q, Zhang R, *et al*. Enhancement of terahertz wave emission from air plasma excited by harmonic three-color laser fields [J]. *Opt. Commun.*, 2021, **481**: 126533.
[29] Wang S F, Xiao H C, Peng Y. Mechanism study of terahertz radiation regulation in a multi-color laser field [J]. *J. Opt. Soc. Am. B*, 2020, **37**(11): 3325-3334.
[30] Alirezaee H, Sharifian M, Darbani S M R, *et al*. Terahertz radiation emission from three-color laser-induced air plasma [J]. *Eur. Phys. J. Plus*, 2020, **135**(4): 342.
[31] Pei M J, Lu C H, Wang X W, *et al*. Enhancement and modulation of terahertz radiation by multi-color laser pulses [J]. *Chin. Phys. B*, 2018, **27**(8): 084209.
[32] Zhang L, Wang G L, Zhao S F, *et al*. Controlling of strong tunable THz emission with optimal incommensurate multi-color laser field [J]. *Phys. Plasmas*, 2017, **24**(2): 023116.
[33] Zhou Z Y, lv Z H, Zhang D W, *et al*. Analysis of THz generation by multicolor laser pulses with various frequency ratios [J]. *Phys. Rev. A*, 2020, **101**(4): 043422.
[34] Rodriguez G, Siders C W, Chunlei G, *et al*. Coherent ultrafast MI-FROG spectroscopy of optical field ionization in molecular H_2, N_2, and O_2 [J]. *IEEE J. Sel. Top. Quant. Electron.*, 2001, **7**(4): 579-591.
[35] Wu P H, Yang C S, Chen P H, *et al*. Optimization of Terahertz Source via an Ambient Air-Based Multi-Color Photoionization [C]. 2019 44th International Conference on Infrared, Millimeter, and Terahertz Waves (IRMMW-THz), IEEE, 2019, 1-2.
[36] Liu S J, Fan Z Q, Lu C H, *et al*. Coherent control of boosted terahertz radiation from air plasma pumped by a femtosecond three-color sawtooth field [J]. *Phys. Rev. A*, 2020, **102**(6): 063522.